COBEM 2023 27TH INTERNATIONAL CONGRESS OF MECHANICAL ENGENEERING

ABCM Brazilian Society of Mechanical Sciences and Engineering
27th ABCM International Congress of Mechanical Engineering
December 04-08, 2023, Florianópolis-SC, Brazil

COB-2023-1126
MODELING AND EVALUATION OF THE REGENERATIVE POTENTIAL OF A QUARTER-CAR WITH HYDRAULIC DAMPER

João Gabriel Benedito Duarte
Augusto Schmidt Lenz
Mariana Damm Poli
Eduardo André Perondi
Universidade Federal do Rio Grande do Sul – Laboratório de Mecatrônica e Controle, Rua Sarmento Leite, 425, Sala 204 – Centro Histórico, Porto Alegre – RS, CEP 90050-170.
joao.benedito@ufrgs.br, augusto.lenz@ufrgs.br, mariana.poli@ufrgs.br, perondi@ufrgs.br

Abstract. *Dumpers are crucial in vehicle suspension systems as they absorb kinetic energy from the car's movement that is dissipated as heat. However, this energy is typically lost and, therefore, not utilized for propulsion, limiting overall energy efficiency. In recent works, researchers have studied regenerative hydraulic dumpers, which can convert part of the dissipated energy into electrical energy for powering the vehicle or storing in batteries. Present study proposes to evaluate power harvest potential in a quarter-car model. Employing road profiles based on ISO 8608:2016 with specific roughness and frequency characteristics, simulation results demonstrated the regenerative hydraulic dumper's ability to convert a significant amount of dissipated energy into usable electricity with rougher surfaces and lower frequencies. This research provides valuable insights into the system behavior under different operating conditions, qualifying further development for significantly reducing transportation's environmental impact while improving overall energy performance.*

Keywords: *Energy Harvesting Systems, Hydraulic Damper, Vehicular Vibrations, Vehicle Suspension Systems.*

1. INTRODUCTION

Currently, automotive industry faces significant challenges regarding energy efficiency and autonomy of commercial vehicles. These challenges include the search for more efficient automotive components, electrification of vehicles, advances in energy storage, weight reduction, improved aerodynamics, and the development of charging infrastructure. Overcoming these challenges requires continuous investments in research and development of innovative technologies (Peng et al., 2016; Sanguesa et al., 2021).

One of the systems being studied to enhance the efficiency of commercial vehicles is the energy regeneration system of the hydraulic suspension system. This system aims to recover the energy usually dissipated by the traditional vehicle's dumpers, converting it into hydraulic energy and subsequently into usable electrical energy. The regeneration of this energy allows for its utilization in other vehicle systems, contributing to a more efficient use of available energy resources (Wang et al., 2016).

In this context, present work aims to develop an energy regeneration system to be applied in the hydraulic suspension of commercial vehicles. By utilizing a hydraulic cylinder connected to a hydraulic circuit with a motor coupled to an electric generator, the goal is to capture and store the energy dissipated by the dumpers. The recovered energy can be employed to power auxiliary vehicle systems, recharge batteries, or provide an extra boost to the main engine. Implementing this system will result in increased energy efficiency, reduced fuel consumption and emissions, and enhanced vehicle autonomy (Zhang et al., 2014).

The automotive industry has been driving research and development in this field, investing significant resources to advance this technology. Through partnerships with universities, research centers, and technology suppliers, studies, testing, and prototyping are being conducted worldwide to improve the efficiency and feasibility of this energy regeneration system (Peng et al., 2016).

Looking ahead, it is expected that the application of this technology in commercial vehicles will become increasingly common. With continuous technological advancements and cost reductions, energy regeneration in hydraulic suspension may become a standard feature in commercial vehicles, contributing to energy efficiency and sustainability (Fang et al., 2013b; Zhang et al., 2014a). Moreover, research and development in this field may pave the way for further innovations and technological solutions that enhance the efficiency and autonomy of commercial vehicles (Abdelkareem et al., 2018).

2. REGENERATIVE ELETROHYDRAULIC MODEL

The mathematical modeling approach used in the electro-hydraulic regenerative model is based on the analysis of mechanical, thermodynamics and fluid dynamics. The objective is to develop a precise model that is capable of describing and predicting the behavior of the electro-hydraulic system, considering the regenerative effects. Present mathematical modeling involves the description of the differential equations that govern the behavior of the system components, such as ducts, accumulators, valves, pistons, hydraulic and electric motors, and transmissions.

2.1 Proposed schematic of the regenerative damping system

Figure 1 shows a regenerative hydraulic damper system, previously used by Guo et al. (2017), Fang et al. (2013a), and Zou et al. (2019). In this system, the vehicle's conventional shock absorber is replaced by a hydraulic cylinder that acts as a pump. A set of directional valves that rectify the volumetric flow rate of the hydraulic fluid is coupled to the hydraulic cylinder, allowing this part to move in only one direction. Portion of this fluid enters a high-pressure accumulator (HP), which attenuates impacts and ensures a more stable working condition for the hydraulic motor and, together with a low-pressure accumulator (LP), guarantees the volumetric flow rate supplying related to the difference between volumes of the rod and rodless chambers related to both sides of the piston. A hydraulic motor (M) - connected to this circuit and responsible for converting hydraulic energy into mechanical energy - is coupled to a mechanical transmission device (gear box, GB) that drives an electric generator (G) responsible for transforming mechanical into electrical energy. In this scheme, the fraction of regenerated energy that is harvested is represented by a dissipative effect related to the resistor characterized by a externa resistance R_e, while R_i and L_i are, respectively, generator internal resistance and inductance.

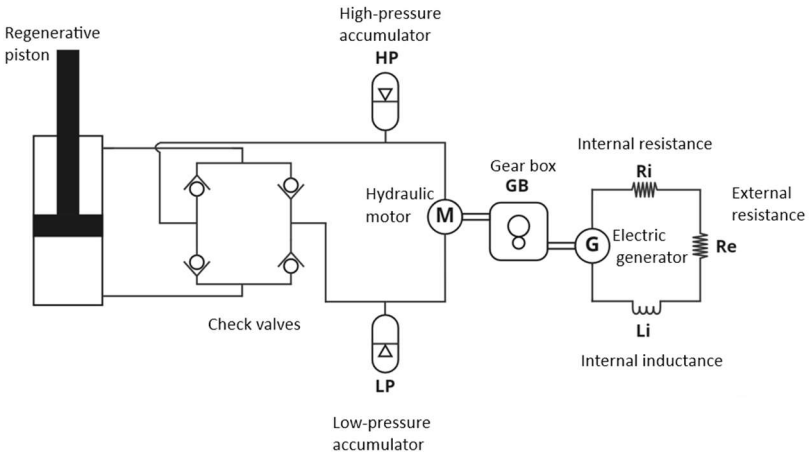

Figure 1. Schematic diagram of the regenerative hydraulic damper system (adapted from Zou et al., 2019).

2.2 Model equations

2.2.1 Quarter-car

A classical quarter-car model is used to model the mechanical suspension system. This model is represented in Gigure (1) and in Table (1) typical parameter used in simulation are presented.

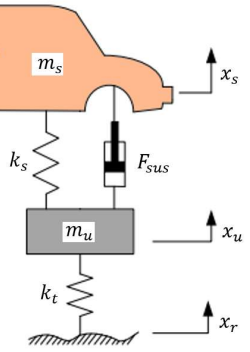

Figure 2. Quarter-car diagram (adapted from Zhou et al., 2018).

Where the variables are:

Table 1. Specification of the parameters of the quarter-car in Figure 1.

Variable	Units	Description
m_s	kg	Suspense mass
m_u	kg	Unsprung mass
k_s	N/m	Suspension elastic constant
k_t	N/m	Tire elastic constant
x_s	m	Position of the suspense mass
x_u	m	Position of the unsprung mass
x_r	m	Position of the road
F_{sus}	N	Force applied by the regenerative system

Considering a quarter-car model for the simulation, the following equations are established:

$$m_s\ddot{x_s} = k_s(x_u - x_s) + F_{sus} \tag{1}$$

$$m_u\ddot{x_u} = k_s(x_s - x_u) + k_t(x_r - x_u) - F_{sus} \tag{2}$$

where m_s is the suspense mass, m_u is the unsprung mass, k_s is the elastic constant of the suspension, k_t is the elastic constant of the tire, x_s is the position of the suspense mass, x_u is the position of the unsprung mass, x_r is the position of the road and F_{sus} is the force applied by the regenerative system as defined in Equation (3):

$$F_{sus} = f(v_p) \tag{3}$$

where v_p is the suspension relative velocity:

$$v_p = \dot{x}_u - \dot{x}_s \tag{4}$$

2.2.2 Hydraulic system

2.2.2.1 Hydraulic piston flow

The hydraulic piston volumetric flow rate is result of two different pump operations, one related to the rod side (Chamber 2) and other elated to the rodless side (Chamber 1). The flows rates of the chambers are given as follows:

$$Q_{b1} = v_p A_1 \tag{5}$$

$$Q_{b2} = -v_p A_2 \tag{6}$$

where Q_{b1} is the volumetric flow rate of Chamber 1, Q_{b2} is the volumetric flow rate of the Chamber 2, A_1 is the area relative to the rodless side and A_2 is the area of the rod side.

2.2.2.2 Accumulators

For taking into account the behavior of the accumulators, the system is divided into two different stages, depending on the sign of the relative velocity of the piston. When the piston is compressing (piston relative velocity greater than zero) the high-pressure accumulator is connected to the Chamber 1, while the low-pressure accumulator is connected to the Chamber 2. This situation is called Case 1. When the piston is expanded (piston relative velocity lower than zero) the high-pressure accumulator is connected to the Chamber 2 while the low-pressure accumulator is connected to Chamber 1. This situation is called Case 2. By using mass conservation principle, in Case 1, the volumetric flow rate into the high-pressure accumulator is given by:

$$Q_{AH} = Q_{b1} - Q_s \tag{7}$$

where Q_{AH} is the volumetric flow rate into the high-pressure accumulator and Q_s is the volumetric flow rate through the hydraulic motor. For the low-pressure accumulator, it is considered:

$$Q_{AL} = Q_{b2} + Q_s \tag{8}$$

where Q_{AL} is the low-pressure accumulator volumetric flow rate. In Case 2, the volumetric flow rate in the high-pressure accumulator is given by:

$$Q_{AH} = Q_{b2} - Q_s \tag{9}$$

And the low-pressure accumulator volumetric flow rate is:

$$Q_{AL} = Q_{b1} + Q_s \tag{10}$$

2.2.2.2.1 High-pressure accumulator

The equation that describes the behavior of the high-pressure accumulator is composed by the conservation of mass on the interface of the accumulator with the hydraulic circuit and an internal polytropic process associated to the gas compression and expansion phenomena. Based in Guo et al. (2017), the polytropic and mass conservation processes can be expressed by:

$$pV^r = const \tag{11}$$

$$V_{AH} = \int J_{AH} dt \tag{12}$$

$$V_{GAH} = V_{iGAH} - V_{AH} \tag{13}$$

where p is a pressure under analysis in a polytropic process, V is the volume under analysis, r is the polytropic index, V_{AH} is the volume of the fluid in the high-pressure accumulator, V_{GAH} is the volume of the gas in the high-pressure accumulator and V_{iGAH} is the initial value for this volume, also, the subindexes $(\,)_{iGAH}$ and $(\,)_{iGAL}$ indicates initial conditions of the i^{th} component. Using the polytropic relation:

$$p_3 {V_{GAH}}^r = p_{iGAH} {V_{iGAH}}^r \tag{14}$$

where p_3 is the pressure of the high-pressure accumulator and p_{iGAH} is the initial pressure in the accumulator. Then, by making replacements and reorganizing, is achieved:

$$p_3 (V_{iGAH} - V_{AH})^r = p_{iGAH} {V_{iGAH}}^r \tag{15}$$

$$V_{AH} = V_{iGAH} - \left[\frac{p_{iGAH} {V_{iGAH}}^r}{p_3}\right]^{\frac{1}{r}} \tag{16}$$

$$\int Q_{AH} dt = V_{iGAH} - V_{iGAH} \left[\frac{p_{iGAH}}{p_3}\right]^{\frac{1}{r}} \tag{17}$$

$$Q_{AH} = -V_{iGAH} {p_{iGAH}}^{\frac{1}{r}} \frac{d}{dt}\left[{p_3}^{-\frac{1}{r}}\right] \tag{18}$$

$$Q_{AH} = V_{GAH} \frac{\dot{p_3}}{r \times p_3} \tag{19}$$

To determine V_{GAH}, we must consider whether the initial pressure of the high-pressure chamber is greater than the pressure on the accumulator in a determined time, the volume of the fluid in the high-pressure accumulator, V_{AH}, will be zero, on the other hand if the pressure p_3 is greater, we can calculate the volume V_{AH} by means Equation (17), according Peng et al. (2019):

$$\begin{cases} V_{AH} = V_{iGAH}\left(1 - \dfrac{p_{iGAH}}{p_3}\right)^{\frac{1}{r}}, & se\ p_{iGAH} \leq p_3 \\ V_{AH} = 0, & se\ p_{iGAH} > p_3 \end{cases} \tag{20}$$

Finally, the volume V_{GAH} can be calculated by:

$$V_{GAH} = V_{iGAH} - V_{AH} \tag{21}$$

2.2.2.2.2 Low-pressure accumulator

The equation that describes the behavior of the low-pressure accumulator is similar to that one of the high-pressure accumulator, therefore:

$$\begin{cases} V_{AL} = V_{iGAL}\left(1 - \dfrac{p_{iGAL}}{p_4}\right)^{\frac{1}{r}}, & se\ p_{iGAL} \leq p_4 \\ V_{AL} = 0, & se\ p_{iGAL} > p_4 \end{cases} \tag{22}$$

Furthermore, the volume V_{GAL} can be calculated by means:

$$V_{GAL} = V_{iGAL} - V_{AL} \tag{23}$$

2.2.2.3 Valves and pressure drop

The use of unidirectional valves results in a pressure drop in the location where they are positioned. The following model is used to describe the pressure reduction:

$$\Delta p = sign(J) J^2 R_V \tag{24}$$

where Δp is the pressure drop, J is the volumetric flow rate and R_V is an estimated linear hydraulic resistance of the valve $R_V\left[\frac{kg}{m^5}\right]$ can be represented by:

$$R_V = K_d^{-2} \tag{25}$$

where K_d is the valve constant, defined by:

$$K_d = C_d A_V \sqrt{\frac{2}{\rho}} \tag{26}$$

where C_d is the discharge factor, A_V is the sectional area of the valve and ρ is the specific mass of the fluid.

2.2.2.4 Hydromechanical system

The hydromechanical system performs the conversion between the volumetric flow rate and pressure in the hydraulic motor to the rotation and torque applied to the generator shaft passing through the gearbox. The hydraulic motor conversion can be expressed by means:

$$\Delta p_{HM} K_{HM} = T_{HM} \tag{27}$$

where K_{HM} is the hydraulic motor constant $\left[\frac{m^3}{rev}\right]$ and T_{HM} is the torque of the hydraulic motor. Adding torques allows to determine the angular velocity of the shaft. Then:

$$T_{HM} - T_E = J_0 \dot{\omega_S}^2 + C_t \omega_S \tag{28}$$

where T_E is the electrical torque given by the generator, J_0 is the mass moment of inertia of the entire rotational system, ω_S is the angular velocity of the shaft and C_t is the viscous friction coefficient. Moment of inertia J_0 can be expressed as a computation of the moments of inertia of the hydraulic motor, gearbox and generator, considering the difference in velocity given by the transformation of the gearbox. J_0 can be calculated by means:

$$J_0 \dot{\omega_S}^2 = J_{HM} \dot{\omega_S}^2 + J_{GB} \dot{\omega_S}^2 + J_G \dot{\omega_G}^2 \tag{29}$$

With:

$$\dot{\omega}_G = \frac{\dot{\omega}_S}{\alpha_{GB}} \tag{30}$$

where J_0 is the total mass moment of inertia, J_{HM} is the mass moment of inertia of the hydraulic motor, J_{GB} is the mass equivalent moment of inertia of the gearbox, J_G is the moment of inertia of the generator shaft and ω_G is the angular velocity of the generator shaft. Operating previous equations we obtain:

$$J_0 = J_{HM} + J_{GB} + \frac{J_G}{{\alpha_{GB}}^2} \tag{31}$$

2.2.3 Electrical system

The power conversion from the hydromechanical to the electrical system is performed by an electric generator, which presents a constant of transformation K_G $[Vs/rad]$, allowing to express the generated electric tension E_g as:

$$E_g = K_G \omega_G \tag{32}$$

As consequence, the generator equation becomes:

$$E_g = R_i i + R_{reg} i + L_i \frac{di}{dt} \tag{33}$$

where R_i is the generator internal resistance, L_i is the generator internal inductance, R_{reg} is the resistance equivalence of the storage system and i is the electrical current intensity. Solving for the current intensity allows to calculate the torque applied to the rotational system with an equivalent generator constant K_G.

$$T_E = K_G i \tag{34}$$

A suitable way to quantify the energy regeneration capability of the system is through the power output at the external resistor, which can be calculated applying:

$$P_{reg} = R_{reg} i^2 \tag{35}$$

2.3 Simulink model

The Simulink model developed for the vehicle suspension with regenerative hydraulic system has proven to be a useful tool for simulating the dynamic behavior of the system. Through simulation, it is possible to evaluate the performance of the suspension in terms of energy efficiency and vehicle dynamic behavior. Figure 2 presents a representative schematic of the simulation model.

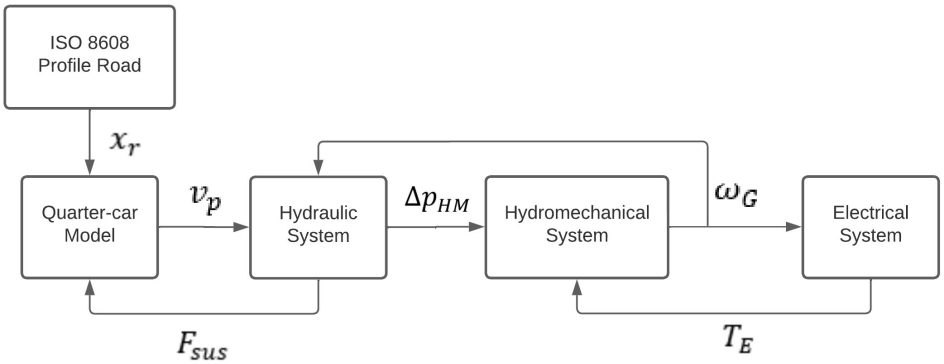

Figure 3. Simulation model diagram.

The parameters values used in the model depicted in Figure 2 are presented in the following tables:

Table 2. Parameters of the quarter-car model.

Variable	Value	Units	Description
m_s	664.5	kg	Vehicle body (Sprung mass)
m_u	31.25	kg	Wheel mass (Unspring mass)
k_s	118000	N/m	Spring stiffness
k_t	1200000	N/m	Tire stiffness

Table 3. Parameters of the hydraulic system.

Variable	Value	Units	Description
R_{VH}	3×10^8	Ns/m^5	Hydraulic resistor
A_1	0.001963	m^2	Larger piston area
A_2	0.001347	m^2	Smaller piston area
J_{HM}	1×10^4	kg.m^2	Hydraulic motor inertia
K_{HM}	3.2×10^5	m^3/rot	Hydraulic motor volumetric capacity
p_i	1×10^5	N/m^2	Initial pressure in the circuit
S	0.22	m	Piston stroke
V_{iGAL}	6×10^3	m^3	Low-pressure accumulator volume
V_{iGAH}	3×10^3	m^3	High-pressure accumulator volume
p_{iGAH}	1×10^5	Pa	Initial internal pressure in the high-pressure accumulator
p_{iGAL}	0.8×10^4	Pa	Initial internal pressure in the low-pressure accumulator
r	1.4	-	Specific heat ratio of the gas
A_V	3.93×10^4	m^2	Block valve area
ρ	872	m^3	Oil density
C_d	0.7	-	Discharge coefficient
K_d	3.194×10^5	m^3(m/kg)$^{0.5}$	Valve constant
R_V	9.974×10^6	m^6/kg	Equivalent hydraulic resistor of the valve

Table 4. Parameters of the electrical system.

Variable	Value	Units	Description
K_G	0.242	N.m/A	Electric motor constant
R_i	3.9	Ω	Generator internal resistor
R_{reg}	Variable	Ω	Regenerative generator resistor
L_i	2.83×10^{-3}	H	Generator internal inductance
J_G	6×10^{-5}	kg.m^2	Generator inertia

Table 5. Parameters of the gear box.

Variable	Value	Units	Description
α_{GB}	1/3.5	-	Reduction constant
J_{GB}	1×10^{-4}	kg.m^2	Reducer inertia
C_t	0.05	Nm/rot	Torque viscous friction coefficient
J_0	1.857×10^{-3}	kg.m^2	Total moment of inertia of the rotating mass

3. SIMULATION AND ANALYSIS

For the model presented in Figure 2, the system power behavior, including hydraulic, mechanical, and electrical subsystems, are presented. Additionally, the RMS value of voltage, regenerated electrical power, body acceleration, and current are determined for a range of external resistor values between 1Ω and 100Ω. Surface profiles A, B, and C are used as inputs to the model, aiming to reproduce real-world terrain conditions. This approach allows for analysis of the system's performance in various scenarios, taking into account the variations in terrain characteristics. The obtained results will provide valuable insights into the system's behavior under different terrain conditions, as well as elucidate the variations in powers and body responses concerning external resistor values.

It is possible to observe in Figure 4 that the proposed regenerative system presents its best efficiency in terms of energy regeneration for external resistance load of 6 Ω. Beyond this resistor value, its energy regeneration capacity decreases. However, it is also possible, in this case, to observe the maintenance of a constant average value of voltage and current.

In the sequence, Figure 5 shows the RMS body acceleration values according to the progressive increase of the external resistor value. This figure indicates that the acceleration of the chassis growths as the load applied to the generator increases. This is due to the fact that the higher the value of the external resistor, the greater the torque required to drive the generator, resulting in stiffening the damper (as shown by Guo et al. (2017)), also decreasing the effective rotor angular velocity. The increase in the load related to the generator creates an additional resistance to the movement, requiring more effort to overcome this resistance effect. This increased torque requirement results in a slower response from the hydraulic suspension, corroborating with the results of Zou et al. (2019).

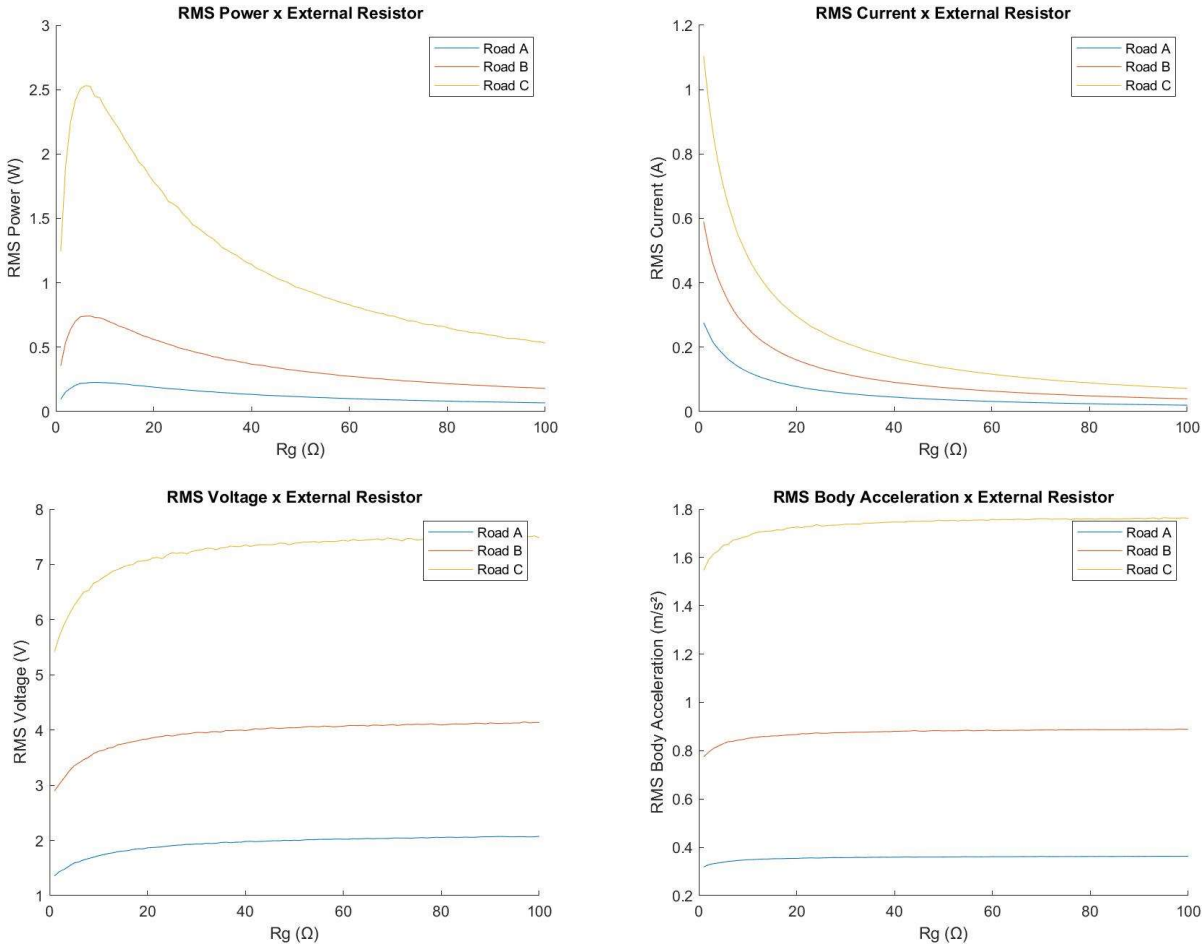

Figure 4. Evaluation of the root mean square (RMS) average of the electrical power, voltage, current and body acceleration values in road profiles A, B, and C for external resistor values between 1 Ω and 100 Ω.

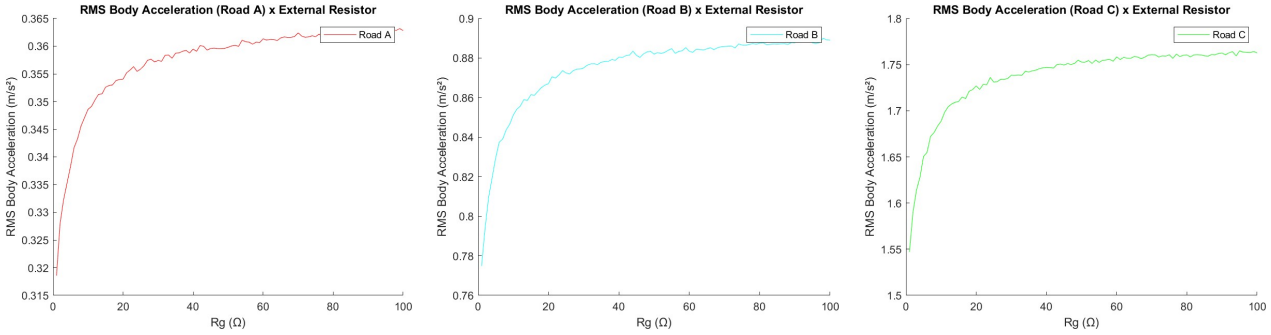

Figure 5. Relationship between body acceleration and external load applied for terrain profiles A, B and C.

Another relevant analysis within the scope of this article is the comparison between the powers of the proposed regenerative system. Figure 6 presents a comparison between two external resistor values (10Ω and 50Ω) for the three road profiles discussed. This analysis allows us to understand the amount of energy available for harvesting in the system, taking into consideration the specific characteristics of the model.

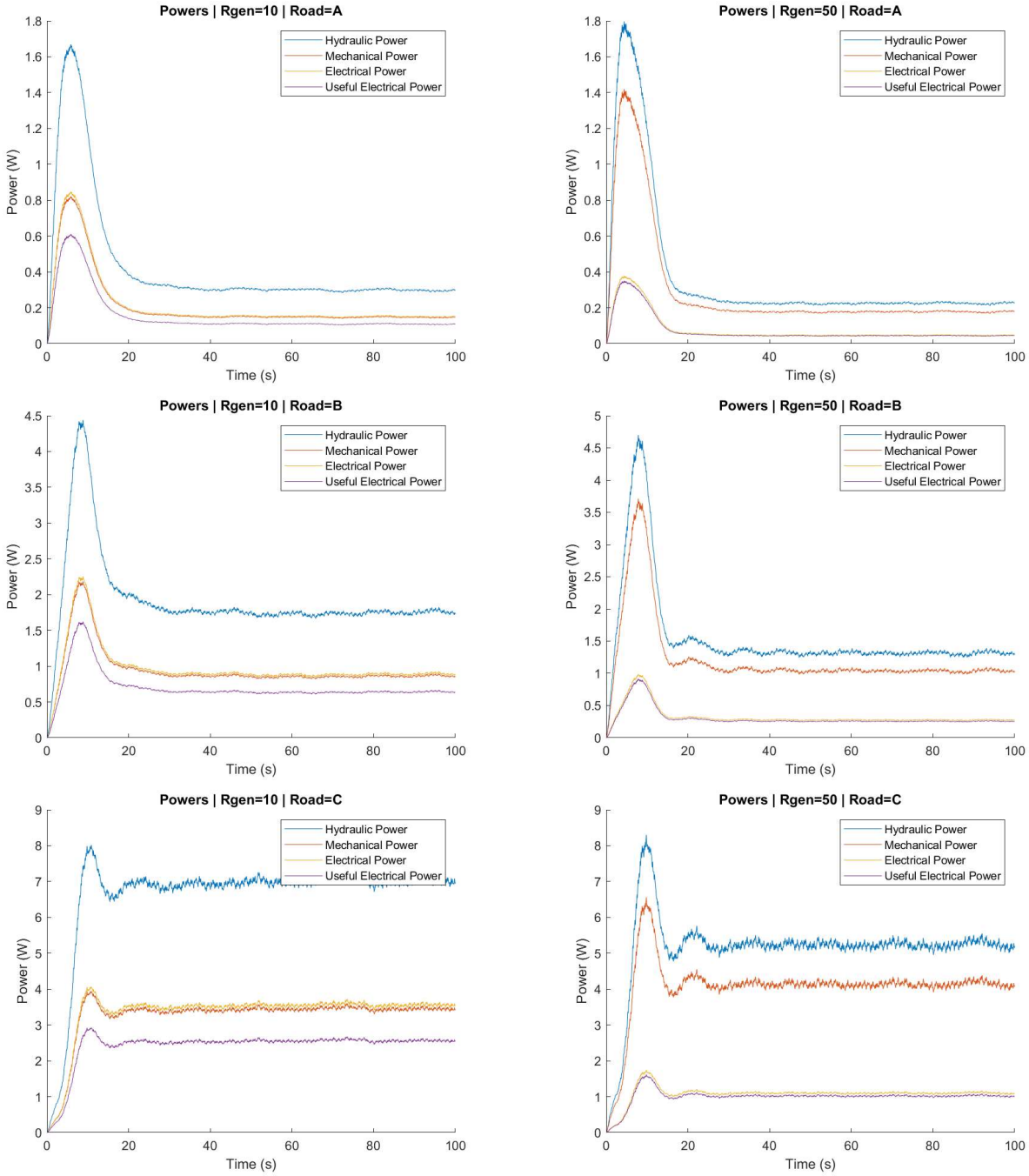

Figure 6. Comparison of the difference between the power outputs of the electrohydraulic system according to the variation of external resistors for values of 10Ω and 50Ω, considering the surface profiles A, B, and C.

The results revealed significant differences in the amount of useful electrical power obtained for different external resistor values and track profiles. The 10Ω external resistor provided a higher amount of available power for utilization, while the 50Ω resistor yielded a lower amount of exploitable power.

Based on the obtained results, we can state that for a regenerative electro-hydraulic system, the load imposed by the generator has a significant influence on the system's dynamic behavior. When the value of the external electrical load is low, the generator is able to convert a greater amount of kinetic energy into electrical energy, while also providing a more responsive chassis to road excitations. However, as the value of the external resistor increases, the system's energy harvesting capacity decreases, resulting in a stiffer suspension. Therefore, as there is a compromise between the energy harvested and the suspension performance, it is important to retrieve a balance in the system configurations in order to accomplish a suitable relation between dynamic response and amount of energy regeneration.

4. CONCLUSIONS

The proposed model enables a clearer understanding of the system, its regenerative capacity, and the dynamic behavior across different road profiles, according to the ISO 8606:2016 Standard. Based on the analysis of simulation data, it was observed that the external load (represented as an equivalent electrical resistance) applied to the generator directly influences the suspension dynamics and, consequently, its regenerative capacity. In this study, it was found that for this system the best external resistor to achieve the highest available useful energy potential is approximately 6 Ω. Values above this resistor resulted in a declining regenerative capacity and an increasing suspension stiffness. In addition to considering the efficiencies and characteristics of the components and the influence of the external load, an important aspect to be addressed in future work is the influence of hydraulic accumulators in the system, investigating the sizing influence of these components in the overall behavior and in the energy regeneration capacity of the system.

5. ACKNOWLEDGEMENTS

The authors would like to thank Universidade Federal do Rio Grande do Sul - UFRGS and Laboratório de Mecatrônica e Controle - LAMECC for their support in the development of this work.

6. REFERENCES

Abdelkareem, M. A. A., Xu, L., Ali, M. K. A., Elagouz, A., Mi, J., Guo, S., et al. (2018). Vibration energy harvesting in automotive suspension system: A detailed review. *Applied Energy,* Vol. 229, p. 672–699. doi: 10.1016/j.apenergy.2018.08.030.

Fang, Z., Guo, X., Xu, L., and Zhang, H. (2013a). An Optimal Algorithm for Energy Recovery of Hydraulic Electromagnetic Energy-Regenerative Shock Absorber. *Applied Mathematics & Information Sciences,* Vol. 7, p. 2207–2214. doi: 10.12785/amis/070610.

Fang, Z., Guo, X., Xu, L., and Zhang, H. (2013b). Experimental Study of Damping and Energy Regeneration Characteristics of a Hydraulic Electromagnetic Shock Absorber. *Advances in Mechanical Engineering,* Vol. 5, p. 943528. doi: 10.1155/2013/943528.

Guo, S., Xu, L., Liu, Y., Guo, X., and Zuo, L. (2017). Modeling and Experiments of a Hydraulic Electromagnetic Energy-Harvesting Shock Absorber. *IEEE/ASME Transactions on Mechatronics,* Vol. 22, p. 2684–2694. doi: 10.1109/TMECH.2017.2760341.

Peng, M., Guo, X., Zou, J., and Zhang, C. (2016). Simulation Study on Vehicle Road Performance with Hydraulic Electromagnetic Energy-Regenerative Shock Absorber. in doi: 10.4271/2016-01-1550.

Sanguesa, J. A., Torres-Sanz, V., Garrido, P., Martinez, F. J., and Marquez-Barja, J. M. (2021). A Review on Electric Vehicles: Technologies and Challenges. *Smart Cities,* Vol. 4, p. 372–404. doi: 10.3390/smartcities4010022.

Wang, R., Gu, F., Cattley, R., and Ball, A. (2016). Modelling, Testing and Analysis of a Regenerative Hydraulic Shock Absorber System. *Energies (Basel),* Vol. 9, p. 386. doi: 10.3390/en9050386.

Zhang, H., Guo, X., Xu, L., and Zhang, J. (2014). Simulation and test for hydraulic electromagnetic energy-regenerative shock absorber. *Nongye Gongcheng Xuebao/Transactions of the Chinese Society of Agricultural Engineering,* Vol. 30, p. 38–46. doi: 10.3969/j.issn.1002-6819.2014.02.006.

Zhou, C., Liu, X., Chen, W., Xu, F., and Cao, B. (2018). Optimal Sliding Mode Control for an Active Suspension System Based on a Genetic Algorithm. *Algorithms,* Vol. 11, p. 205. doi: 10.3390/a11120205.

Zou, J., Guo, X., Abdelkareem, M. A. A., Xu, L., and Zhang, J. (2019). Modelling and ride analysis of a hydraulic interconnected suspension based on the hydraulic energy regenerative shock absorbers. *Mech Syst Signal Process,* Vol. 127, p. 345–369. doi: 10.1016/j.ymssp.2019.02.047.

7. RESPONSIBILITY NOTICE

The authors are the only responsible for the printed material included in this paper.